

FINAL RESULTS ON AN EXPERIMENT TO DETERMINE THE LOWER TEMPERATURE LIMIT OF VOID SWELLING OF STAINLESS STEELS AT RELATIVELY LOW DISPLACEMENT RATES –

S. I. Porollo, Y. V. Konobeev, A. M. Dvoriashin, and V. M. Krigan (Institute of Physics and Power Engineering, Obninsk, Russia) and F. A. Garner (Pacific Northwest National Laboratory)*

OBJECTIVE

The objective of this effort is to determine the lower temperature limit of void swelling when reactor components are exposed to relatively low displacement rates.

SUMMARY

Recent studies associated with light water reactors (LWR) in both the USA and Russia have raised the question of void swelling in austenitic components of core internals. One question of particular interest is the range of temperatures over which voids can develop, especially the lowest temperature. This question is equally relevant to fusion reactors, especially those operating with water cooling and therefore exposed to temperatures below those attainable in various high-flux fast reactors used to generate most of the relevant high fluence data.

To address this question a flow restrictor component manufactured from annealed X10H18T was removed from the reflector region of the BN-350 fast reactor. During operation this component spanned temperatures and dpa rates of direct interest not only to pressurized water reactors (PWRs) in the West and VVERs in Russia, but also to various proposed fusion devices. This steel is analogous to AISI 321 and is used in Russian reactors for applications where AISI 304 would be used in the West. This component was sectioned on a very fine scale to determine in what range of conditions voids existed. Microstructural data were obtained for 157 separate locations, with 111 specimens showing voids over the relevant range of temperatures and displacement rates, allowing construction of a parametric map of swelling with temperature, dpa and dpa rate. These data show that void swelling at 10 to 50 dpa persists down to ~306°C for dose rates in the range 0.1×10^{-7} to 1.6×10^{-7} dpa/sec.

Introduction

Voids as a new type of radiation defect were discovered in fuel pin cladding made from austenitic stainless steels irradiated in the DFR fast reactor (Cawthorne and Fulton, 1967). For a long time it was perceived that the phenomenon of void formation is characteristic only for fast reactor irradiation with its high displacement rates and elevated irradiation temperatures. Recently data have become available providing evidence that void formation may occur in structural materials of PWR and VVER internals, in which neutron damage doses of 50 dpa and higher can be accumulated during operating lifetimes. In addition to dimensional changes, swelling in structural materials of PWR and VVER internals (in particular, austenitic stainless steels such as AISI 304 and X18H10T) will lead to appearance of mechanical stresses caused by the non-uniformity of swelling and can also lead to irradiation embrittlement if the swelling level exceeds some critical value.

As a rule, the temperature dependence of swelling in austenitic steels such as X18H10T and other metals and alloys often exhibits a bell-shaped form with a maximum, height and location of which are determined by the initial microstructural condition of a material, but especially by irradiation conditions. Specifically, the most important parameters are the inlet and outlet temperatures of the reactor component and the neutron flux profile across the reactor, which for small reactors is often bell-shaped. The actual low temperature limit of void formation in a material should be related to low vacancy mobility and/or to the ability of vacancies to aggregate and form voids, a condition that may exist below the inlet temperature of a given reactor. Likewise, the upper temperature limit of void formation is usually related to a low super-saturation of vacancies at high temperatures, often well above the maximum temperature of the material in any given reactor.

Data on swelling of steels such as X18H10T in fast reactors are reasonably available. However, most

* Pacific Northwest National Laboratory (PNNL) is operated for the U.S. Department of Energy by Battelle Memorial Institute under contract DE-AC06-76RLO-1830.

of these data have been obtained for neutron irradiation temperatures above 350-370°C, and only scarce data on swelling are available for temperatures in the range 280 - 350°C. The same can be said concerning data for the austenitic steel 304, which is a steel of type X18H9 in the Russian notation. The reason is simply that most Western and some Russian fast reactors have relatively high inlet sodium temperatures, on the order of 365°C or higher.

Experimental data on swelling in austenitic stainless steels irradiated at temperatures below 350°C at dose rates relevant to PWRs and VVERs are of significant interest, since the inlet temperatures of these reactors is usually below 300°C. Potential sources of such data are core components and internal devices of pressurized water reactors, but it is often very difficult to remove components from such devices at high enough neutron exposure. Such devices usually operate at much lower flux levels than used in fast reactors.

Another approach is to examine components of fast reactor cores irradiated to high doses with inlet temperatures significantly lower than 350°C. This approach introduces a significant influence of neutron flux when the components are extracted from the core region. A third and better approach is to examine a very long-lived component from the low-flux reflector region of a fast reactor with a low inlet temperature, which is the path used in this study.

In this report the results are presented of a microstructural study to determine the swelling of type 12X18H9T austenitic stainless steel after irradiation in the BN-350 fast reactor at temperatures ranging from 280°C to 334°C and doses from 9 to 56 dpa. Extensive sectioning of the component followed by electron microscopy was the approach employed.

This effort is now complete after four years duration. Several earlier reports presented fractions of these data as it was collected (1,2).

Material and irradiation conditions

To study the swelling and mechanical properties of type 12X18H9T steel after low-temperature neutron irradiation, one of the BN-350 components was chosen. This component served as a coolant flow restrictor in the line connecting the reactor vessel to a sodium tank. The component is a hexagonal tube of 96 mm flat-to-flat size, having a central cylindrical hole of 65 mm in diameter. The total length of the flow restrictor component equals the length of reference driver subassemblies of the BN-350 fast reactor (3.435 m). This flow restrictor component was made from type 12X18H9T austenitic stainless steel of nominal composition (wt. %): C ≤ 0.12; Cr -17-19. Ni -8-9.5; Mn ≤2; Si ≤0.8; Ti -0.5-0.7. The (wt.%) composition was checked using an x-ray micro-analyzer "Kamebax" and was found to be Cr - 18.5; Ni - 9.5; Mn - 1.5; Si - 0.6-0.8; Ti -0.6-0.7. Thus, the steel composition corresponds to the nominal specification.

The component was exposed without replacement or rotation for 46,536 h (from November, 1972 till June, 1984) in the BN-350 core at the radial distance of 94.5 cm from the core axis. The maximum neutron fluence at the core midplane was equal to 3.3×10^{23} n/cm² (E>0) or 1.6×10^{23} n/cm² (E>0.1 MeV). These fluences correspond to maximum neutron damage dose of 56 dpa at a maximum dose rate of 3.34×10^{-7} dpa/s. The relative values of the total and fast neutron fluence as well as dose in the component are shown in Figure 1.

The calculated distribution of irradiation temperatures for both nearest and farthest flats from the core axis is shown in Table 1. The distribution of irradiation temperature in the component was calculated at the average level of reactor capacity equal to 60% nominal reactor capacity for the period from 1973 to 1984. The inlet sodium temperature was 280°C. Throughout the irradiation period the average heating of sodium in surrounding subassemblies of the lateral breeder zone was ~60°C.

Cutting of specimens

From the data shown in Table 1 it follows that in each section of the component there is a complicated distribution of dose, neutron fluence and irradiation temperature. Due to different cooling conditions the maximum difference of temperature between internal and outer component surfaces reaches

Table 1. The distribution of irradiation temperature (°C) in different cross sections of the flow restrictor component

Distance from midplane, mm	Outer surface, inboard flat	Internal surface, inboard flat	Outer surface, outboard flat	Internal surface, outboard flat
-750	282	282	281	281
-450	290	287	288	286
-150	306	296	303	293
0	317	302	313	299
+150	324	304	321	301
+450	334	307	333	306
+750	337	307	336	306

30°C. The neutron fluence and dose between two arbitrary points in a cross section of the component may differ by factor of two and more.

In the hot cell of the BN-350 site the central section of the flow restrictor component was cut into 5 pieces, each of 300 mm length. The pieces designated #1, #3 and #5 (see Figure 2) corresponding to the bottom, middle and top parts of the component, were transported to the hot laboratory of IPPE. In Figure 2 a map is presented illustrating the accessible dose-temperature irradiation conditions for each component section. The areas of the map corresponding to absent pieces 2 and 4 are shaded. As seen in Figure 2., the accessible area of dpa and irradiation temperatures has a complicated form and is limited by doses of 4 and 56 dpa and irradiation temperatures of 282 and 335°C. Since the dpa-temperature areas corresponding to different pieces of the component overlap partially, this allows one to get some information that one would otherwise like to obtain from lost pieces #2 and #4.

To obtain the most complete information on swelling the scheme of cutting of TEM specimens shown in Figure 3 was chosen. To prepare specimens for electron microscopy investigation (disks of 3 mm in diameter and of 0.3-0.4 mm in thickness) several samples were cut out from each corner of the component (7 specimens) and from the middle of each face (5 specimens). The scheme of cutting of TEM specimens shown in Figure 3 was realized for three cross sections located at distances of 0, -150 and +590 mm from the core midplane. For the cross section located at the distance of -670 mm, TEM specimens were cut out only from three faces. Such a scheme of cutting the TEM specimens allowed us to fill rather uniformly the area of the dpa-irradiation temperature map with sufficient experimental points (shown as crosses in Figure 2).

Microstructure and swelling of 12X18H9T stainless steel

Data on irradiation conditions and swelling for the cross sections located at distances of -670, -150 and 0 mm from the core midplane are shown in Table 2. In Figure 4 the dose-irradiation temperature map of the void formation in type 12X18H9T stainless steel is shown. Out of 157 conditions examined, 111 specimens were found to contain voids.

The microstructure of 12X18H9T steel in the sections investigated is characterized by the presence of voids, dislocation loops, dislocation segments, two types of precipitates, and deformation stacking faults. Voids were observed in sections -150, 0 and +590 (Figure 5), but no voids were detected in sections -670 and -450 mm. The void characteristics are listed in Table 2.

The dislocation structure of the irradiated steel consists of both faulted and perfect dislocation loops and linear dislocations (Figure 6). The total length of dislocations per unit volume depends only slightly on the irradiation temperature.

In the irradiated steel two types of precipitates were observed. The first type are spherical particles with the mean diameter of 58.7 nm and concentration of $5.0 \times 10^{14} \text{ cm}^{-3}$. The volume fraction of these precipitates equals 0.72%. From electron diffraction patterns it appears that the diffraction reflections most likely correspond to TiC precipitates, most probably formed in the steel during solidification. It

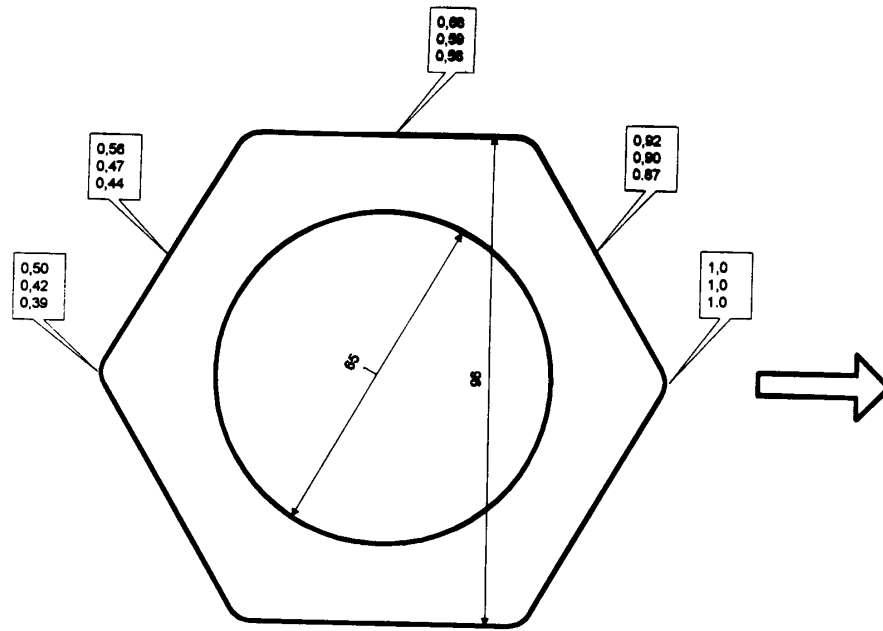


Figure 1. Normalized distribution (listed from the top downward) of neutron fluences $E > 0$ and $E > 0.1$ MeV and dpa dose over cross section of the BN-350 flow restrictor component. The arrow points toward the core axis.

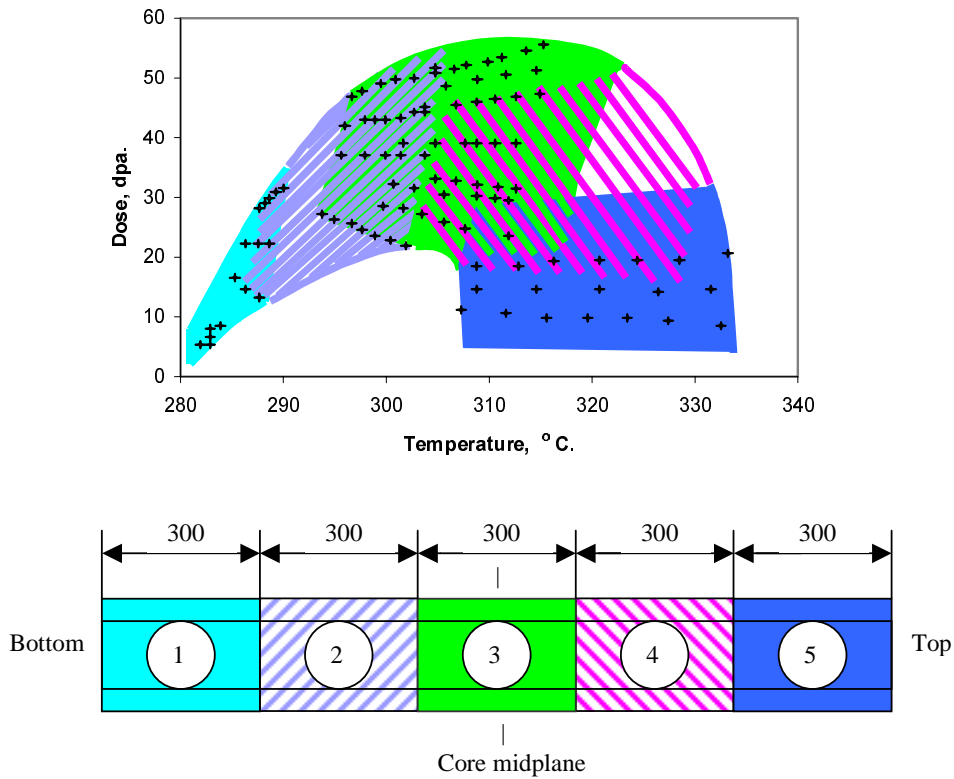


Figure 2. The dose-temperature map of irradiation conditions and the scheme of initial cutting of the flow restrictor component (lengths in mm).

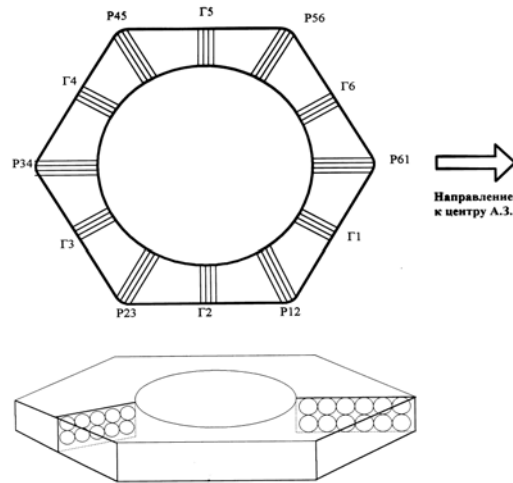


Figure 3. The scheme of cutting the TEM- specimens for component cross-sections located at distances of 0, -150 and +590 mm from the core midplane. P and Г are derived from the Russian words for “corner” and “face” respectively. The Russian under the arrow note that it points to the core axis.

Table 2. Microstructural data for the 12X18H9T steel

Sample number	Dose. dpa	Temperature °C	Mean void diameter. nm	Void concentration. 10^{14} cm^{-3}	Void volume fraction. %
-150_P34.1	21.6	302	4.4	Voids in single grains	
-150_P56.3	43.4	302	4.9	0.82	0.0008
-150_P56.3	43.6	302	4.9	0.8	0.001
-150_P61.3	50.3	302	5.1	1.2	0.001
-150_P56.2	43.8	303	4.9	1.9	0.002
-150_P56.2	44	303	4.9	1.9	0.002
-150_P56.1	42.2	304	4.4	1.4	0.00144
-150_P61.2	51.2	304	5.0	1.4	0.02
-150_P56.1	44.5	305	4.4	1.4	0.0014
-150_P61.1	52.1	305	4.8	1.7	0.02
0_P34.4	25.7	306	7.9	1.5	0.006
0_Г4.3	30.5	306	5.2	0.5	0.001
0_P23.4	32.5	307	6.4	0.78	0.002
0_P56.5	45.5	307	4.7	1.96	0.002
0_P61.5	51.7	307	4.7	1	0.001
+750_P34.7	4.5	308	9.9	28	0.23
590_P34.7	10.0	308	9.4	8.4	0.06
+590	10.3	308	8.1	12.6	0.056
+590_P34.7	10.3	308	9.4	8.4	0.06
0_P34.3	24.8	308	9.2	3.1	0.02
0_Г2.3	39.2	308	5.4	0.84	0.001
0_Г5.3	39.2	308	5.3	0.52	0.001
0_P61.4/5	52.1	308	4.9	0.9	0.001
+750_P61.7	7.9	309	10.7	21	0.19
590_Г5.5	13.7	309	9.5	6	0.04

590_Г2.5	13.7	309	8.0	6	0.03
+590_Г2.5	14.1	309	8.3	6	0.03
+590_Г5.5	14.1	309	9.5	6.3	0.04
590_61.7	17.5	309	9.0	8	0.05
+590_P61.7	18	309	9.0	7.9	0.05
0_Г4.2	29.9	309	6.0	0.91	0.002
0_P23.3	32.0	309	8.1	1.2	0.006
0_Г2.2/5	39.2	309	5.4	0.78	0.001
0_P56.4	45.9	309	6.2	4.7	0.01
0_Г1.3	49.8	309	6.0	1.08	0.002
+750_Г2.5	6.2	310	9.7	14	0.1
0_P61.4	52.6	310	5.0	1.4	0.002
0_Г4.1/5	29.5	311	7.0	2.1	0.007
0_P23.2	31.6	311	8.5	2.9	0.013
0_Г2.2	39.2	311	6.6	1.7	0.004
0_Г5.2	39.2	311	6.6	1.8	0.005
0_P56.3	46.4	311	6.2	4.75	0.01
+750_P34.6	4.4	312	11.8	36	0.46
+590_P34.6	9.9	312	9.0	21	0.12
+590	10.0	312	7.0	6	0.002
+590	10.3	312	7.5	9	0.003
0_P34.1	23.0	312	9.0	7.1	0.044
0_Г3.1	29.2	312	8.7	0.28	0.001
0_Г4.1	29.2	312	8.0	2.6	0.012
0_Г1.2	50.6	312	6.6	2.7	0.006
0_P61.3	53.6	312	5.9	4.5	0.009
+750_P61.6	8.1	313	10.9	27	0.25
+590_P61.6	18.3	313	10.1	22	0.19
0_P23.1	31.1	313	9.1	2.1	0.013
0_Г2.1	39.2	313	8.7	0.85	0.004
0_Г5.1	39.2	313	7.2	8.6	0.024
0_P56.2	46.8	313	6.9	13.9	0.037
0_P61.2	54.5	314	6.7	10	0.026
+590	10.0	315	8.6	19	0.09
+590_Г2.4	14.1	315	9.0	15	0.09
+590_Г5.4	14.1	315	10.4	18	0.16
0_P56.1	47.3	315	7.0	15.8	0.049
0_Г6.1	51.4	315	7.1	7.9	0.021
+750_Г2.4	6.2	316	14.0	15	0.3
+590_P34.5	9.6	316	11.0	38	0.4
0_P61.1	55.4	316	7.1	9.2	0.024
+750_P34.5	4.2	317	12.8	33	0.53
+590_P61.5	18.6	317	11.4	20	0.24
+750_P61.5	8.2	318	11.1	27	0.27
+590	9.4	319	10.5	19	0.09
+590_P34.4	9.3	320	13.1	37	0.65
+590	18.7	320	10.5	20	0.18
+750_P34.4	4.1	321	13.7	23	0.60
+590_Г2.3	14.1	321	10.4	19	0.18
+590_Г5.3	14.1	321	11.8	22	0.3
560	16.8	321	12.4	12	0.17
+590	18.9	321	9.9	25	0.18
+590_P61.4	19	321	12.5	27.5	0.44
+750_Г2.3	6.2	322	14.5	18	0.4
+750_P61.4	8.4	322	11.2	21	0.23
+590_P34.3	8.9	324	14.0	27	0.6

+750_P34.3	3.9	325	18.0	22	0.9
+590_P61.3	19.3	325	14.2	22	0.5
+750_P61.3	8.5	326	16.5	16	0.5
+590	9.5	327	13.7	18	0.38
+590_Г2.2	14.1	327	11.1	29	0.32
+590_Г5.2	14.1	327	12.8	21	0.35
+750_Г2.2	6.2	328	15.4	19	0.53
+590_P34.2	8.6	328	18.0	25	0.95
590_P34.2	8.4	329	18.0	25	0.96
+590_P61.2	19.6	329	14.0	21	0.45
+750_P61.2	8.7	331	17.2	16	0.6
+750_P34.2	3.8	332	18.3	19	0.9
+590_P34-Г4	8.4	332	16.9	22	0.69
+590	8.9	332	14.5	26	0.57
+590	9.4	332	12.3	31	0.43
+590_Г5.1	14.1	332	15.0	24	0.67
+590_Г2.1	14.1	332	13.8	22	0.47
590	14.5	332	17.3	6.4	0.28
590_P34.1	8.1	333	18.0	18	0.77
+590_P34.1	8.3	333	17.0	20	0.70
590_Г2.1	13.7	333	14.0	22	0.50
590_Г5.1	13.7	333	15.0	24	0.70
+750_Г2.1	6.2	334	20.0	10	0.5
590_P61-Г1.1.4	18.8	334	16.7	18	0.65
590_P61-Г1.1.3	19.0	334	14.4	22	0.50
590_61.1	19.4	334	17.0	14	0.50
+590	19.8	334	12.4	28	0.43
+590_P61.1	19.9	334	17.0	14	0.49
+750_P61.1	8.8	335	17.3	16	0.6

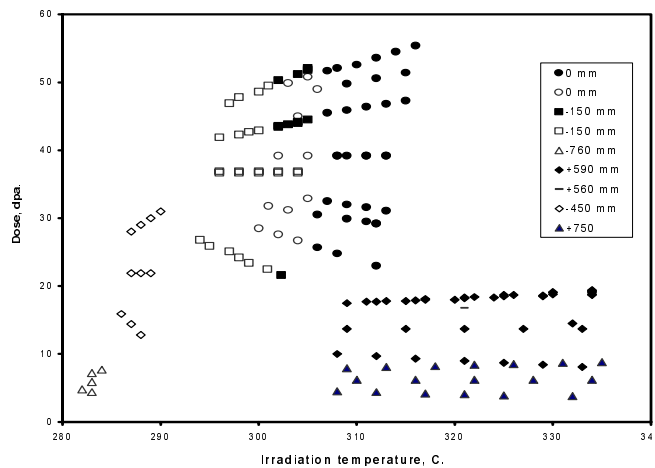
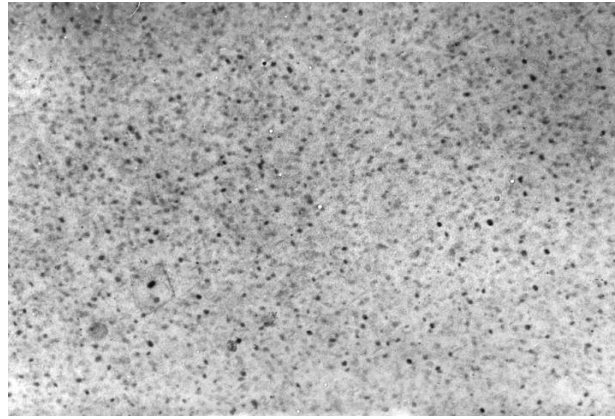
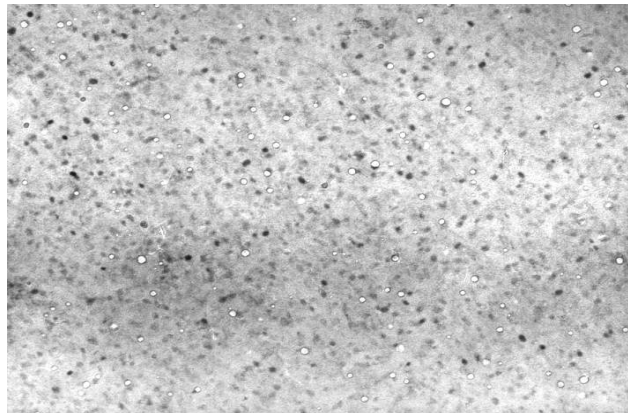


Figure 4. The dose-irradiation temperature map of void formation in the 12X18H9T steel irradiated in BN-350. Filled symbols indicate that voids were observed, and empty symbols signify no voids were present.

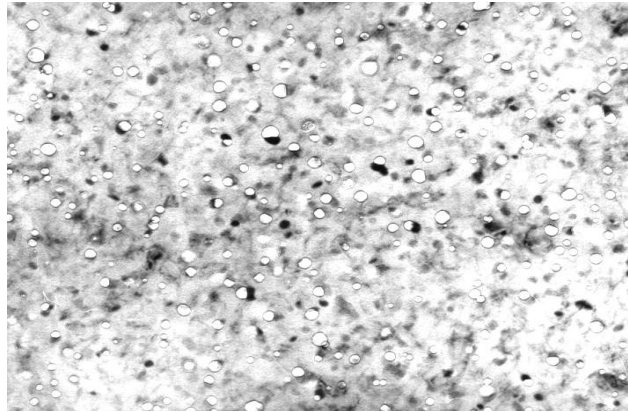
should be noted that this type of precipitate is observed in all investigated sections of the flow restrictor component. Another type of precipitate is much smaller, finely dispersed precipitates in the grain interior (Figure 7). Analysis has shown that these precipitates are G-phase, most likely induced by irradiation.



a)



b)



c)

Figure 5. Voids in 12X18H9T steel after neutron irradiation: a) at 302°C to 50.3 dpa, b) at 308°C to 10.3 dpa, and c) at 324°C to 8.9 dpa. $\times 100,000$.

Along with the defects mentioned above, flat stacking faults were observed in the irradiated steel (Figure 8), probably, due to deformation of TEM specimens during handling and thinning.

Results and discussion

In Figures 9 - 12 the temperature dependence of the mean void diameter $\langle d_v \rangle$, void concentration N_v , void volume fraction and product $\langle d_v \rangle N_v$ are shown. Despite significant scatter within the data field, it

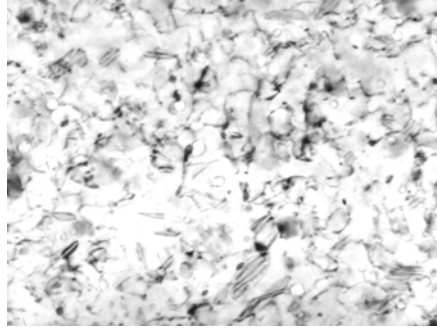


Figure 6. Dislocation structure of the 12X18H9T steel after neutron irradiation at 329°C to 19.6 dpa (cross section at +590 mm).

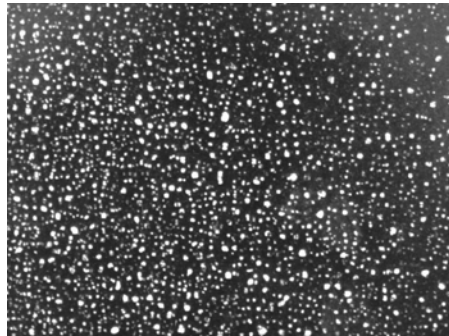
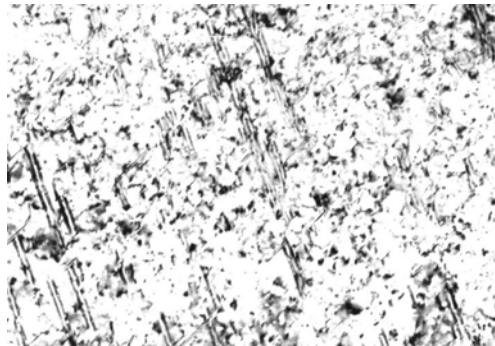
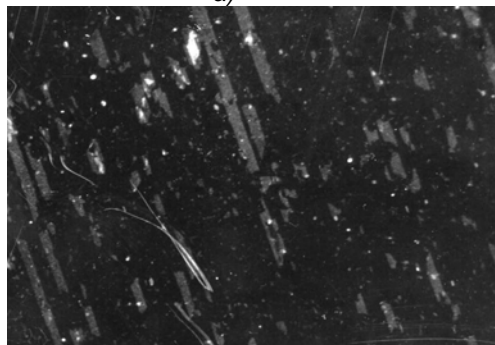


Figure 7. G-phase precipitates in the 12X18H9T steel after neutron irradiation: at 302°C to 27.6 dpa (cross section at 0 mm).



a)



b)

Figure 8. Deformation stacking faults in the 12X18H9T steel after neutron irradiation at 314°C to 54.5 dpa (cross section at 0 mm). a) bright-field image, b) dark-field image.

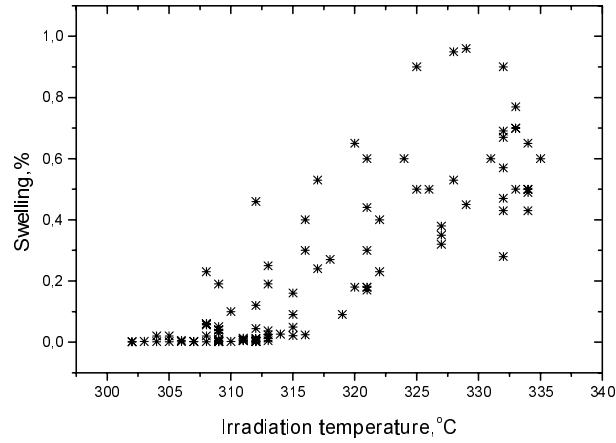


Figure 11. Temperature dependence of void swelling.

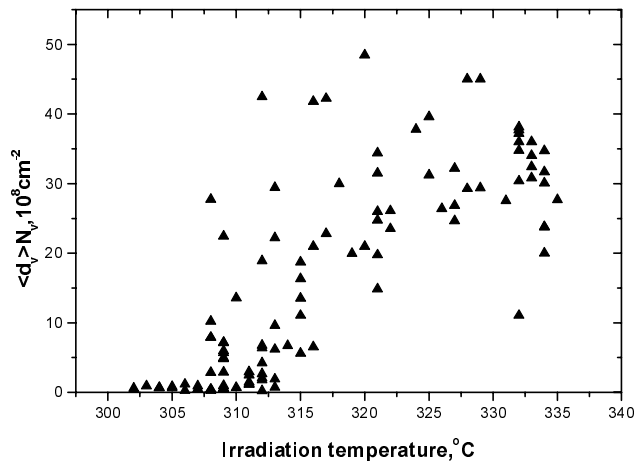


Figure 12. Temperature dependence of the product $\langle d_v \rangle N_v$, determining the contribution of voids to the yield strength increment in the 12X18H9T steel.

Figure 13 shows that one of the major sources of data scatter arises from the flux dependence of void swelling. Note that when relatively small ranges of temperature are chosen, swelling appears to decrease with increasing dpa. This is a counterintuitive observation, but is consistent with the results of several recent studies showing that increases in the dpa rate delay the onset of accelerated swelling (4-6).

Another conclusion concerning the temperature range of void swelling can be seen in Figure 14 when comparing the swelling data from the flow restrictor with those data published earlier in various Russian journals, but derived from the BR-10 fast reactor. The inlet temperature of BR-10 during this period was $\sim 420^\circ\text{C}$. It is obvious that the peak swelling temperature in BR-10 reflects more the peak in the flux profile across this relatively small core. The lower temperature limit of void swelling is only an artifact of the inlet temperature.

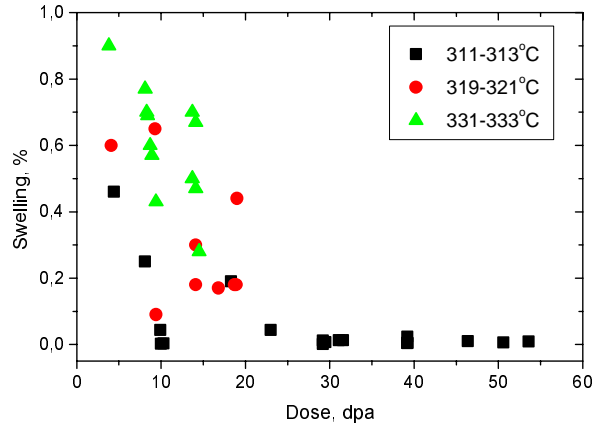


Figure 13. Dependence of swelling on temperature, dpa and dpa rate for selected small increments of temperature. Since the dpa rate is proportional to the dpa level in this constant time experiment, the data also suggest a strong dependence of swelling on dpa rate.

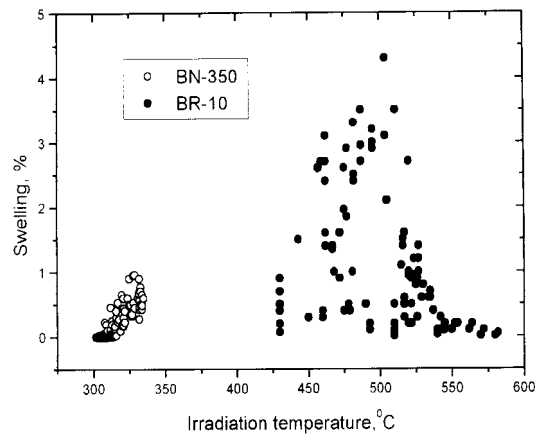


Figure 14. Comparison of swelling data for two fast reactors with very different inlet temperatures.

The lower temperature limit observed in the flow restrictor data set, however, is most likely a real lower limit determined by the severely limited vacancy migration at such a low temperature, and it is quite likely that there is a continuum in swelling not observable in the temperature range shown in Figure 14.

Conclusions

On the basis of the present microstructural study it is possible to make the following conclusions.

1. Voids in type 12X18H9T austenitic steel irradiated in the BN-350 fast reactor at dose rates ranging from 1.6×10^{-7} dpa/s to 3.1×10^{-7} dpa/s were observed in the temperature range of 302-334°C at doses ranging from 26.3 to 55.4 dpa. At lower irradiation temperatures voids resolvable by electron microscopy were not found, even though the dpa level approaches 50 dpa.
2. The mean void diameter increases monotonically with increasing neutron irradiation temperature in the range of 302°C - 334°C, from 4.4 - 5.1 nm at doses ranging from 22 to 50 dpa to 14.4 - 17.0 nm at doses of 19-20 dpa.
3. At the temperature of 330°C and doses ranging from 8 to 20 dpa the swelling is between 0.3 and 1.0 %.

4. There appears to be some support in this data set to expect a reduction in swelling as the dpa rate increases, consistent with the results of other studies.

REFERENCES

- [1] S. I. Porollo, A. N. Vorobjev, Yu. V. Konobeev, A. M. Dvoriashin, and F. A. Garner, "The Influence of PWR-Relevant Atomic Displacement Rates and Temperatures on Void Swelling in the Russian Equivalent of AISI 304 Stainless Steel", *International Symposium on "Contribution of Materials Investigation to the Resolution of Problems Encountered in Pressurized Water Reactors*, 14-18 Sept. 1998, Fontevraud, France, pp. 271-280.
- [2] S. I. Porollo, Yu. V. Konobeev, A. M. Dvoraishin, V. M. Krigan and F. A. Garner, "Determination of the Lower Temperature Limit of Void Swelling of Stainless Steels at PWR-relevant Displacement Rates", *10th International Conference on Environmental Degradation of Materials in Nuclear Power Systems – Water Reactors*, 2001, in CD format only. Also published in Fusion Materials Semiannual Progress Report for Period Ending June 30, 2001, pp. 111-126.
- [3] J. P. Robertson, I Ioka, A. F. Rowcliffe, M. L. Grossbeck and S. Jitsukawa, "Temperature Dependence of the Deformation Behavior of Type 316 Stainless Steel After Low Temperature Neutron Irradiation", *Effects of Radiation on Materials: 18th International Symposium, ASTM STP 1325*, R.E. Nanstad, M.L. Hamilton, F.A. Garner, and A.S. Kumar, Eds., American Society for Testing and Materials, West Conshohocken, PA, 1999, pp. 671-688.
- [4] T. Okita, N. Sekimura, F. A. Garner, L. R. Greenwood, W. G. Wolfer and Y. Isobe, "Neutron-Induced Microstructural Evolution of Fe-15Cr-16Ni Alloys at ~400°C During Neutron Irradiation in the FFTF Fast Reactor", *10th International Conference on Environmental Degradation of Materials in Nuclear Power Systems – Water Reactors*, 2001, in CD format only.
- [5] G. M. Bond, B. H. Sencer, F. A. Garner, M. L. Hamilton, T. R. Allen and D. L. Porter, "Void Swelling of Annealed 304 Stainless Steel at ~370-385°C and PWR-Relevant Displacement Rates", *9th International Conference on Environmental Degradation of Materials in Nuclear Power Systems – Water Reactors*, 1999, pp. 1045-1050.
- [6] F. A. Garner, M. L. Hamilton, D. L. Porter, T. R. Allen, T. Tsutsui, M. Nakajima, T. Kido, T. Ishii, G. M. Bond and B. H. Sencer, to be submitted to *Journal of Nuclear Materials*.